

Forschungszentrum Karlsruhe
Technik und Umwelt

Wissenschaftliche Berichte
FZKA 6066

MHD Flows in Thick-walled Ducts

L. Bühler

**Institut für Angewandte Thermo- und Fluidodynamik
Projekt Kernfusion**

Mai 1998

Forschungszentrum Karlsruhe

Technik und Umwelt

Wissenschaftliche Berichte

FZKA 6066

MHD flows in thick-walled ducts

L. Bühler

Institut für Angewandte Thermo- und Fluidodynamik
Projekt Kernfusion

Forschungszentrum Karlsruhe GmbH, Karlsruhe
1998

**Als Manuskript gedruckt
Für diesen Bericht behalten wir uns alle Rechte vor**

**Forschungszentrum Karlsruhe GmbH
Postfach 3640, 76021 Karlsruhe**

**Mitglied der Hermann von Helmholtz-Gemeinschaft
Deutscher Forschungszentren (HGF)**

ISSN 0947-8620

MHD flows in thick-walled ducts

L. Bühler

Abstract

The magnetohydrodynamic flow in ducts with infinitely thick walls is investigated. The flow is evaluated by an asymptotic analysis valid for strong magnetic fields. The solution for current and potential in the wall is obtained by the solution of an integral equation. For the special case of a circular pipe the results are confirmed by the use of conformal mapping. It is found that in circular pipes the velocity profile is of slug type. In square ducts high-velocity jets are possible. These jets may be located along the diagonal or along the side walls if the diagonal or the side walls are aligned with the magnetic field, respectively. The pressure drop depends essentially on the conductivity of the walls and may be considerably lower than in perfectly conducting ducts.

MHD Strömungen in dickwandigen Kanälen

L. Bühler

Zusammenfassung

Magnetohydrodynamische Strömungen in Kanälen mit unendlich dicken Wänden werden mittels asymptotischer Berechnungen für starke Magnetfelder untersucht. Die Lösung für den elektrischen Strom und das elektrische Potential in der Wand wird auf die Lösung einer Integralgleichung zurückgeführt. Für den Sonderfall eines Kreisrohres können die Ergebnisse anhand konformer Abbildungen überprüft werden. Man findet im Kreisrohr ein kolbenförmiges Geschwindigkeitsprofil. In quadratischen Kanälen sind starke Geschwindigkeitsüberhöhungen möglich. Diese befinden sich lokalisiert in engen Bereichen, entweder entlang der Diagonalen oder entlang von Seitenwänden, sofern das Magnetfeld parallel zur Diagonalen oder parallel zu den Seitenwänden ausgerichtet ist. Der Druckverlust hängt wesentlich von der Leitfähigkeit der Wände ab und kann Werte erreichen, die erheblich niedriger sind, als die in perfekt leitenden Kanälen.

Contents

1	Introduction	3
2	Formulation	4
3	Analysis	6
3.1	The Hartmann layers	6
3.2	The duct wall	7
3.3	The core	8
3.4	The side layers	9
4	Applications	11
4.1	Circular pipes	11
4.2	Square duct, diagonally aligned with the field	15
4.3	Square duct, side walls aligned with the field	17
5	Conclusions	20

1 Introduction

Liquid-metal blankets for nuclear fusion reactors under current investigation use the liquid metal Li or the alloy LiPb as breeding materials. According to actual designs the liquid breeder is supplied to the blanket through relatively small channels drilled in very thick steel plates. Even if the overall velocity in the blanket required for a Tritium removal is small, the velocities in the supplying channels can reach considerable values. Due to its electric conductivity the fluid exerts strong interaction with the magnetic field applied for the fusion plasma confinement. In the moving fluid electric currents are induced which generate Lorentz forces opposing the flow and thus create the main part of pressure drop. One method to keep the pressure drop within acceptable limits is to reduce the electric currents by choosing thin duct walls with high Ohmic resistance for the closure of the current loops. Unfortunately this is in contradiction with the current engineering design and thus motivates the present analysis.

In the past, magnetohydrodynamic (MHD) channel flows have been investigated within the scope of self-cooled fusion blankets. In order to reduce pressure drop, the metallic walls have been designed as thin as possible and a number of results for flows in such ducts with thin walls are available. Far from being complete, some of these works should be mentioned here for a short overview. Chang and Lundgren (1961) already present solutions in thin-walled conducting ducts with arbitrary cross section, including the special case of a circular duct previously considered by Shercliff (1956). For rectangular ducts the papers by Hunt (1965) and Walker (1981) are among the most cited works in this field. The latter theory has been extended to account for flows in rectangular ducts with variable cross section in the same paper. MHD flows in non-uniform fields, in bends, in multiple, electrically coupled channels or in general geometries and magnetic fields have been considered e.g. by Ting, Hua, Walker and Picologlou (1993), Moon, Hua and Walker (1991), Molokov and Bühler (1994), Molokov (1993), Bühler (1994).

Up to now, flows in ducts with thick conducting walls have been estimated conservatively as if the duct walls had infinite conductivity. By this assumption the potential inside the walls is uniform and has not to be determined during the analysis. The flow becomes of slug type and, in appropriate scales (see later in this paper), the pressure drop reaches unity.

The present work will show that for wall conductivities comparable to that of fluid the pressure drop will be roughly the half as predicted by the conservative approach. If the wall conductivity is smaller than that of the fluid, even smaller values for pressure drop are possible. The velocity distribution in ducts with finite conductivity may deviate considerably from that predicted by the conservative estimates. Calculations show that high-velocity side layer jets along walls aligned with the magnetic field are possible. This has not been expected (by the author and not predicted by the conservative approach) but becomes obvious by considering the problem in detail. For square ducts diagonally aligned with the magnetic field internal high velocity layers are found. In both cases the layers are relatively thin, even if their thickness and flow rates are on the order one.

2 Formulation

The stationary, fully developed flow of an electrically conducting fluid within a strong, externally applied uniform magnetic field $B\hat{\mathbf{y}}$ is governed by the equations for conservation of momentum

$$M^{-2}\nabla^2\mathbf{v} + \mathbf{j} \times \hat{\mathbf{y}} = \nabla p, \quad (1)$$

mass

$$\nabla \cdot \mathbf{v} = 0, \quad (2)$$

charge

$$\nabla \cdot \mathbf{j} = 0, \quad (3)$$

and Ohm's law

$$\mathbf{j} = -\nabla\phi + \mathbf{v} \times \hat{\mathbf{y}}, \quad (4)$$

where $\hat{\mathbf{y}}$ is the unit vector in magnetic field direction and \mathbf{v} , \mathbf{j} , ϕ and p represent the velocity, electric current density, electric potential, and pressure scaled by the reference quantities v_0 , $\sigma v_0 B$, $v_0 B L$, and $\sigma v_0 B^2 L$, respectively. The reference value for the velocity is chosen as the mean value and L is a characteristic dimension of the duct cross section. In dimensionless units the duct extends in magnetic field direction over a length of 2 (see figure 1).

The only nondimensional group is the Hartmann number

$$M = BL\sqrt{\frac{\sigma}{\rho\nu}}. \quad (5)$$

The electric conductivity of the fluid σ , the density ρ , and the kinematic viscosity ν are assumed to be constant. The square of the Hartmann number gives the ratio of electromagnetic and viscous forces.

At the fluid-wall interface Γ there is no-slip, continuity of wall-normal currents and potential,

$$\left. \begin{array}{l} \mathbf{v} = 0, \\ \mathbf{j} \cdot \hat{\mathbf{n}} = \mathbf{j}_w \cdot \hat{\mathbf{n}}, \\ \phi = \phi_w, \end{array} \right\} \text{ on } \Gamma \quad (6)$$

if there is no contact resistance between fluid and wall. The unit normal to the wall is denoted by $\hat{\mathbf{n}}$. The subscript "w" indicates properties in the wall.

It is assumed in the following analysis that the wall material is conducting. Currents which leave the fluid enter the wall and create there a potential distribution according to

$$\mathbf{j}_w = -\sigma_w \nabla \phi_w, \quad (7)$$

where σ_w stands for the ratio of wall to fluid conductivity. The wall is assumed to be much thicker than the dimension of the duct cross section. Currents close their circuit on distances of the order one, decaying quickly at larger distances from the duct center so that

$$\mathbf{j}_w \rightarrow 0 \text{ as } r = \sqrt{y^2 + z^2} \rightarrow \infty. \quad (8)$$

For a definition of coordinates see figure 1.

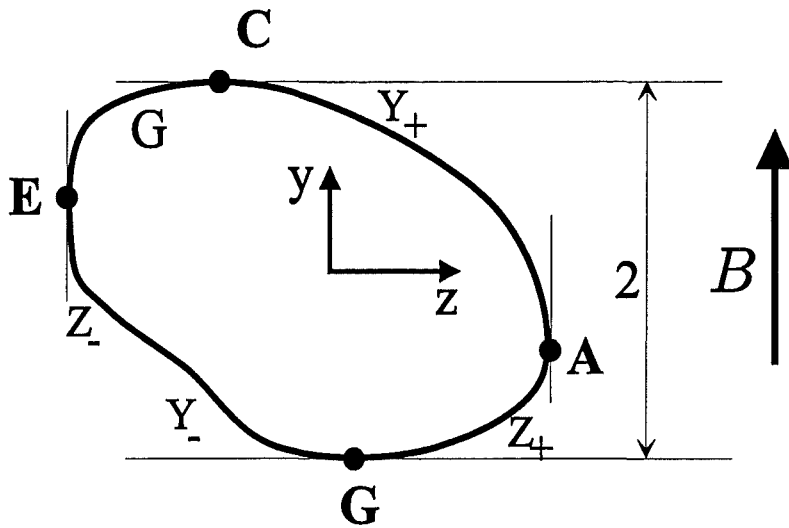


Figure 1: Sketch of the duct cross section. The y coordinate coincides with the direction of the magnetic field. The flow direction is along x and points into the normal direction of this figure. The scale is chosen such that the maximum and minimum position in y are ± 1 . The fluid-wall interface Γ may be split into the parts $Y(z)_{\pm}$ connecting the points A and E or into the parts $Z(y)_{\pm}$ connecting C and G .

3 Analysis

Fully developed flows are characterized by a uniform pressure gradient $\nabla p = -K$, a unidirectional velocity $\mathbf{v} = u\hat{\mathbf{x}}$ and vanishing derivatives of other variables along the duct axis. The governing equations in the fluid reduce to

$$\left. \begin{aligned} M^{-2}\nabla^2 u + K &= j_z, \\ j_z &= -\partial_z \phi + u, \\ j_y &= -\partial_y \phi. \end{aligned} \right\} \quad (9)$$

Conservation of charge requires that

$$\partial_y j_y + M^{-2}\partial_z \nabla^2 u = 0. \quad (10)$$

In the wall the currents are given by

$$j_{wy} = -\sigma_w \partial_y \phi_w, \quad j_{wz} = -\sigma_w \partial_z \phi_w. \quad (11)$$

If the Hartmann number is large, $M \gg 1$, the flow exhibits distinct subregions. One is the core where viscous effects are unimportant. The flow is governed here by a balance between the driving pressure gradient and by the breaking Lorentz forces. The other subregions are the viscous layers near the duct walls. At walls where the magnetic field has a significant normal component normal to the wall the viscous layers are called the *Hartmann layers*. Their thickness scales as $\delta_H \sim M^{-1}$. Along walls which are perfectly aligned with the magnetic field layers of different quality appear. They are known as *side layers* or as parallel layers with typical thickness $\delta_s \sim M^{-1/2}$ (see e.g. Hunt (1965), Walker (1981)). For rectangular ducts with thin conducting walls the side layers can carry an $O(1)$ portion of flow rate at very high velocities proportional to $M^{1/2}$. If the duct walls approach perfectly conductance these side layer jets disappear. Other types of near-wall layers are found in circular ducts near the sides where the magnetic field is tangential to the duct wall. These layers are called here the Roberts layers. Their thickness scales as $\delta_R \sim M^{-1/3}$ while their extension along field lines is $l_R \sim M^{-2/3}$ Roberts (1967). It is known that these layer do not affect the solution in the core and in the Hartmann layers at leading order. Therefore, they are not considered in detail in the following analysis.

All variables are split into the core values plus additional contributions by the viscous Hartmann layers

$$(\mathbf{v}, \mathbf{j}, \phi) = (\mathbf{v}, \mathbf{j}, \phi)_c + (\mathbf{v}, \mathbf{j}, \phi)_H + (\mathbf{v}, \mathbf{j}, \phi)_s. \quad (12)$$

Subscripts "c", "H" and "s" denote fluid variables in the core, in the Hartmann layers and in the side layers, if the latter ones are present in the problem under consideration.

3.1 The Hartmann layers

Firstly, the discussion focuses on the description of the flow in the viscous Hartmann layers. With the stretched coordinate in the Hartmann layer

$$\eta = \pm M (y - Y_{\pm}) \quad \text{with } Y_{\pm} \text{ on } \Gamma \quad (13)$$

the equations (9) reduce to

$$\left. \begin{aligned} \partial_{\eta\eta} u_H - u_H &= 0, \\ \partial_{\eta} \phi_H &= 0. \end{aligned} \right\} \quad (14)$$

as $M \rightarrow \infty$. The variables Y_{\pm} denote the y -positions of the upper and lower fluid-wall interface Γ . Since the viscous contributions have to vanish when approaching the core as $\eta \rightarrow -\infty$ the solutions satisfying all other boundary conditions read

$$u_H = -u_c e^{\eta}, \quad \phi_H = 0. \quad (15)$$

The velocity decays exponentially from the core value to zero when approaching the wall. The electric potential is uniform across the Hartmann layer. To the leading order of approximation there is no viscous correction to this variable. Therefore, the boundary conditions for electric potential can be applied directly to the core variables in the further analysis. If $\sigma_w \gg M^{-1}$, when the duct walls are much better conducting than the Hartmann layers the viscous corrections to the currents vanish as well, $j_{zH} = j_{yH} = 0$, up to the leading order of approximation.

3.2 The duct wall

In the subsection above it has been shown that there are no viscous corrections to the electric core variables at leading order. Therefore, the core values can be directly applied at the duct wall if $M \gg 1$ and $\sigma_w \gg M^{-1}$. Under these assumptions the current density in the fluid core is uniform and already known from the inviscid (or the outer) solution of equation (9a) as

$$j_{cz} = K. \quad (16)$$

If the duct is assumed to be symmetric with respect to $y = 0$, equation(10) leads to

$$j_{cy} = 0. \quad (17)$$

In the wall the charge conservation and Ohm's law lead to the Laplace equation

$$\nabla^2 \phi_w = 0. \quad (18)$$

Instead of directly using this equation a streamfunction ψ for currents is introduced first to explain the main ideas of the following analysis. In terms of ψ the components of currents read

$$j_{wz} = -\sigma_w \partial_z \phi_w = -K \partial_y \psi, \quad (19)$$

$$j_{wy} = -\sigma_w \partial_y \phi_w = K \partial_z \psi, \quad (20)$$

and of course, the Laplace equation $\nabla^2 \psi = 0$ holds.

At the fluid-wall interface the current streamfunction in the wall takes the values as inside the duct,

$$\psi = -y \quad \text{on } \Gamma. \quad (21)$$

At large distances the currents vanish

$$\psi = 0 \quad \text{as } r \rightarrow \infty. \quad (22)$$

A very efficient way in solving the wall solution is by introducing the complex potential F

$$F(\xi) = \varphi + i\psi \quad (23)$$

depending on the complex variable $\xi = z + iy$ ($i = \sqrt{-1}$). The solution for the electric potential ϕ_w is obtained from equation (23) as

$$\phi_w = \frac{K}{\sigma_w} \varphi. \quad (24)$$

The variables ψ and φ are unique for any pressure drop or wall conductivity and depend only on the geometry of the duct.

It is possible to construct a suitable solution for current in the wall by distributing singularities (sources and sinks $dF = -\frac{1}{2\pi} q(s) \ln(\xi - \xi_\Gamma) ds$) along the duct surface where $q(s) ds$ is the source/sink intensity. The solutions which will be derived below have direct physical meaning only inside the wall. Inside the domain which is occupied by the fluid the solutions give "artificial" values which are created by the fact that some "artificial" current is flowing inside the fluid domain between the sources at one side and the sinks at the other side.

The overall solution for the complex potential becomes determined by the integral

$$F = -\frac{1}{2\pi} \oint_{\Gamma} q(s) \ln[\xi - \xi_\Gamma(s)] ds. \quad (25)$$

The complex coordinate ξ is that of arbitrary points in the wall while ξ_Γ stands for points on the fluid-wall interface Γ , denoted by the parameter s ; ($0 \leq s \leq 1$). Note, the solution of F in the wall is independent of the wall conductivity as long as the wall is much better conducting than the Hartmann layers, if $\sigma_w \gg M^{-1}$. The unknown source/sink intensity has to be determined using the equations (21, 23, 25) by the solution of the integral equation

$$-y = -\text{Im}\{\xi_0\} = -\frac{1}{2\pi} \text{Im} \left\{ \oint_{\Gamma} q(s) \ln[\xi_0 - \xi_\Gamma(s)] ds \right\}, \text{ with } \xi_0 \text{ on } \Gamma. \quad (26)$$

With the value of ξ_0 on Γ the equation displayed above has to be integrated with care to avoid singularities.

$$\text{Im}\{\xi(s_0)\} = \frac{1}{2\pi} \lim_{\varepsilon \rightarrow 0} \text{Im} \left\{ \int_0^{s_0-\varepsilon} (\dots) ds + \int_{s_0+\varepsilon}^1 (\dots) ds \right\} \text{ for } \xi(s_0) \text{ on } \Gamma \quad (27)$$

The equation (25) displayed above is valid in the whole wall. The potential at the fluid-wall interface is obtained for values of ξ on Γ . With this result the electric boundary conditions for the fluid are entirely prescribed.

3.3 The core

Finally, the flow in the core is investigated in more detail. The equation (9c) leads directly to the result that the potential in the fluid core is a linear function along

magnetic field lines fixed at the walls by the wall potentials $\phi_{w\pm}$ which lie on the same magnetic field line. The values of $\phi_{w\pm}$ can be calculated directly using equation (24) with $y = y_{\pm}$. For any y symmetric duct j_y vanishes so that $\phi_c = \phi_{w+} = \phi_{w-}$.

The equation (9b) determines the core velocity

$$u_c = K (1 + \sigma_w^{-1} \partial_z \phi_c). \quad (28)$$

If the duct walls are perfectly conducting the velocity becomes uniform in the whole cross section. For walls with a finite conductivity a variation of the core velocity with the z coordinate is possible.

For a determination of the pressure drop the equation (28) has to be integrated over the whole cross section. This leads to the pressure drop given by

$$K = \frac{1}{1 + \sigma_w^{-1} \alpha} \quad (29)$$

where

$$\alpha = \frac{\int_{-1}^1 [\varphi(z_+) - \varphi(z_-)] dy}{\int_{-1}^1 [z_+ - z_-] dy}, \quad \text{with } z_+(y), z_-(y) \text{ on } \Gamma. \quad (30)$$

The parameter α which has been introduced for convenient notation has the order unity, and depends on the shape of the duct. One can identify the well-known result that in perfectly conducting ducts the pressure gradient becomes unity as $\sigma_w \rightarrow \infty$. However, if the duct wall has a finite value of conductivity (as usual in engineering applications) the pressure drop becomes much lower. The conductivity of the metal walls and of the fluid are of the same order of magnitude. This reduces the pressure drop to the half value of that in perfectly conducting ducts but even larger reductions are possible depending on σ_w . This result is most important for applications in fusion engineering, where pressure drops in thick-walled ducts have been overestimated in the past by the values as expected in perfectly conducting ducts. If the duct walls are not infinitely thick there is an additional reduction of pressure drop due to a further increase of the Ohm's resistance in the wall.

3.4 The side layers

During the last subsections solutions for MHD flows in ducts of any arbitrary symmetric cross section has been derived. It has been assumed that the core is entirely surrounded by Hartmann layers at all walls. This restriction excludes the analysis from being applied to rectangular ducts which have one pair of walls aligned with the magnetic field. In such rectangular ducts another type of near-wall boundary layer is found, called the side layer. The side layers of thickness $\delta_s \sim M^{-1/2}$ appear along walls aligned with the magnetic field. They are present at walls near z_+ and z_- , at the right and left side of the duct. With the stretched side layer coordinate

$$\zeta = \pm M^{1/2} (z - z_{\pm}) \quad \text{with } z_{\pm} \text{ on } \Gamma \quad (31)$$

the equation (10) with equations (9b, 9c) lead immediately to the equation determining the side layer contribution of the potential;

$$\partial_{\zeta}^4 \phi_s = \partial_{yy} \phi_s. \quad (32)$$

Toward the core the solution has to match smoothly the core values, $\phi_s = \partial_\zeta \phi_s = 0$ as $\zeta \rightarrow -\infty$. At the side wall the potential is equal to the side wall potential, $\phi_c + \phi_s = \phi_w$ at $\zeta = 0$, and the condition $\partial_\zeta \phi_s = -M^{-1/2}u_c$ at $\zeta = 0$ ensures no slip. The equation above with corresponding boundary conditions is valid if the duct walls are much better conducting than the side layers, when $\sigma_w \gg M^{-1/2}$.

The general solution for ϕ_s which satisfies the boundary condition at the Hartmann walls and the matching condition towards the core is

$$\phi_s = \sum [A_k \cos(\alpha_k \zeta) + B_k \sin(\alpha_k \zeta)] e^{\alpha_k \zeta} \cos(\beta_k y), \quad (33)$$

with

$$\beta_k = \frac{1}{2}k\pi \quad \text{and} \quad \alpha_k = \sqrt{\beta_k/2} \quad \text{for} \quad k = 1, 3, 5, \dots \quad (34)$$

The velocity is obtained from Ohm's Law using $u_s = M^{1/2} \partial_\zeta \phi_s$ as

$$u_s = M^{1/2} \sum \alpha_k [(A_k + B_k) \cos(\zeta) + (B_k - A_k) \sin(\alpha_k \zeta)] e^{\alpha_k \zeta} \cos(\beta_k y). \quad (35)$$

The coefficients are obtained by applying the boundary conditions at $\zeta = 0$.

$$\sum A_k \cos(\beta_k y) = \phi_w - \phi_c. \quad (36)$$

$$\sum \alpha_k (A_k + B_k) \cos(\beta_k y) = M^{-1/2} u_c \quad (37)$$

The A_k are the Fourier coefficients of the difference between the side wall and the core potential, the values $\alpha_k (A_k + B_k)$ are the Fourier coefficients of $M^{-1/2}$ times the core velocity u_c . The solution above has been derived here for the side wall at z_+ . Similar expressions can be obtained for other side wall as well.

The flow rate carried by one side layer is obtained via an integration of Ohm's law across the layer thickness. The integral flow rate in the layer $U_s(y, z_\pm)$ is defined as

$$U_s = M^{-1/2} \int_{-\infty}^0 u_s d\zeta = \pm (\phi_w - \phi_c) \quad \text{at} \quad \zeta = 0, \quad z = z_\pm. \quad (38)$$

4 Applications

In the following subsections results are derived for the flow in a circular duct and in square ducts. Having most general applications in mind, the integral equation (26) determining the source/sink distribution $q(s)$ is solved numerically. For the special case of a circular duct numerical results are confirmed by analytical ones which may be obtained using conformal mapping.

The duct contour is approximated by a finite number n of piecewise linear line elements $\Delta\Gamma_i$ with endpoints ξ_{i-1} and ξ_i . Within one surface element the source intensity, further called q_i , is assumed to be constant. With these assumptions a finite part of the complex potential is determined by an analytical integration of the equation (25) along $\Delta\Gamma_i$ as

$$\Delta F_i = -\frac{1}{2\pi} q_i \frac{\Delta\xi_{w,i-1} \ln(\Delta\xi_{w,i-1}) - \Delta\xi_{w,i} \ln(\Delta\xi_{w,i})}{\Delta\xi_{i,i-1}}. \quad (39)$$

The entire complex potential is finally approximated as the finite sum

$$F = \sum_{i=1}^n \Delta F_i. \quad (40)$$

The variables $\Delta\xi_{w,i-1}$ and $\Delta\xi_{w,i}$ stand for the differences between an arbitrary position ξ_w inside the wall and the endpoints of the line element ξ_{i-1} and ξ_i . The complex distance between the endpoints of the line element is measured with $\Delta\xi_{i,i-1} = \xi_i - \xi_{i-1}$. With these definitions the integral equation (26) leads to a $n \times n$ linear algebraic system for the unknown q_i .

$$y_j = \frac{1}{2\pi} a_{j,i} q_i, \quad 1 \leq i, j \leq n, \quad (41)$$

with

$$a_{j,i} = \frac{\Delta\xi_{j,i-1} \ln(\Delta\xi_{j,i-1}) - \Delta\xi_{j,i} \ln(\Delta\xi_{j,i})}{\Delta\xi_{i,i-1}}. \quad (42)$$

The possible singularity during the solution of the integral equation (see equation (27)) does not occur within this procedure.

In the following the theory described above is applied to some geometries commonly used in engineering. One is the circular tube. The other is the square duct with firstly, one diagonal aligned with the field and secondly, with one pair of walls parallel to the field.

4.1 Circular pipes

Results for current streamlines and isolines of wall potential for a circular pipe

$$\xi_\Gamma = e^{i2\pi s} \quad (43)$$

are shown in the figures 2a and 2b. Currents that leave the duct at z_+ close their path in the wall along circles with the z axis as a tangent. Isolines of potential form an orthogonal set to the current streamlines.

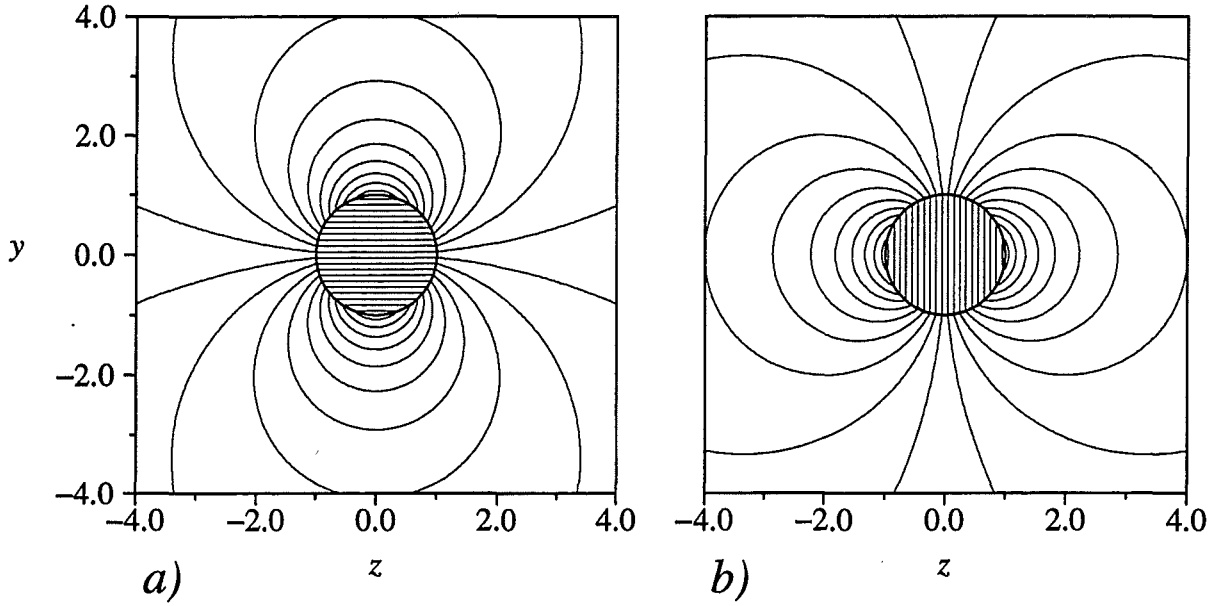


Figure 2: Isolines for current function (a) and potential (b) for the MHD flow in a circular duct with infinitely thick walls. Current lines and isopotential lines in the wall are circles with the x and y axis as a tangent at the origin.

The results described just above may be explained using conformal mapping. Suppose that the solution for core current is known inside the circular pipe and given by the complex potential

$$F = \varphi' + i\psi = -z - iy \text{ inside } \Gamma, \quad (44)$$

then the solution of the problem by conformal mapping is as follows: The physical plane is the plane $\xi_1 = z + iy$. The fluid domain $|\xi_1| < 1$ inside the circle may be mapped to the left half-plane in ξ_2 by the conformal linear rational mapping (see figure 3)

$$\xi_2 = \frac{\xi_1 + 1}{\xi_1 - 1}. \quad (45)$$

All points on Γ in ξ_1 are mapped to the points on the y_2 axis. The points $A-H$ in both planes illustrate clearly how the mapping is performed. The origin O and the infinitely far point in ξ_1 are transformed to the points -1 and 1 in ξ_2 , respectively. The solid straight lines inside Γ representing the core solution in ξ_1 are mapped to the parts of circles shown as solid lines in the left half of ξ_2 . It is now possible to identify the core solution for streamfunction on the y_2 axis as

$$\psi(y_2) = -2 \frac{y_2}{y_2^2 + 1} \quad (46)$$

It was the previous aim to find a source distribution on Γ . Sources and sinks are mapped to sources and sinks of same intensity

$$q(s) ds = q(y_2) \frac{dy_2}{ds} ds. \quad (47)$$

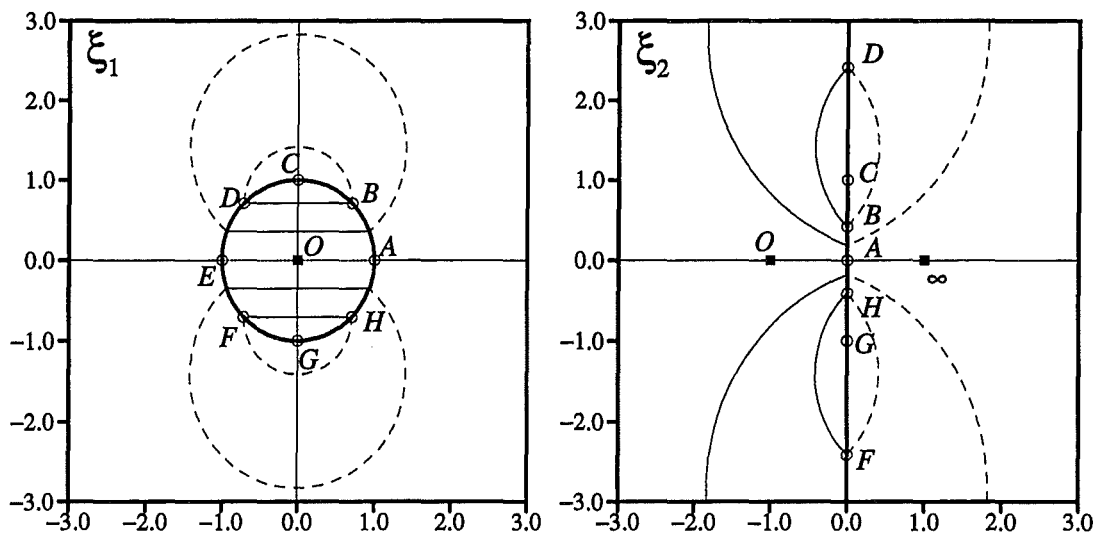


Figure 3: Conformal mapping of a circular duct. The inside and outside of the duct is mapped to the left and to the right half-plane, respectively. The fluid-wall interface Γ becomes the y_2 axis. Current streamlines for the core solution are drawn as solid lines. The dashed lines are the solution in the wall.

Sources are now located on the y_2 axis releasing one half of their intensity to the right, the other half to the left just by symmetry. The change in streamfunction along y determines the source intensity..

$$q(y_2) = 2 \frac{d\psi}{dy_2} \quad (48)$$

Combining the equations (46, 47, 48) one can evaluate the source distribution

$$q(s) = 4\pi \cos(2\pi s). \quad (49)$$

This is an important result since this analytic solution of the integral equation (26) can be used to verify the numerical procedure.

By symmetry the streamlines in the left half-plane (solid) and those in the right half-plane (dashed) must be symmetric with respect to the y_2 axis. That fact leads graphically to the solution inside the wall (the right half-plane in ξ_2). Note that sources between G and C lead virtually to an inversion of the current direction inside the duct producing there a potential distribution $\varphi = z$. The virtual electric potential inside the fluid domain is given then by $\phi = K\varphi$. At the fluid-wall interface the virtual potential corresponds to the physical value of potential since it has the same value as the potential at the wall $\phi_w = K\varphi$ on Γ . The back transformation given by the inversion of equation (45) maps the dashed lines to the wall solution in the physical space, shown as dashed lines in the ξ_1 plane.

Using the symmetry in the ξ_2 plane one can find that $F(\xi_{2,inside}) = -F(\xi_{2,outside})$, where $\xi_{2,outside} = -\xi_{2,inside}$, and on back transformation

$$\xi_{1,outside} = \frac{1}{\xi_{1,inside}}. \quad (50)$$

The solution in the wall is determined by the inversion at the unit circle of core current streamlines with the complex potential given by $F(\xi_{1,outside}) = -F(\xi_{1,inside})$.

$$F = \varphi + i\psi = \frac{1}{z + iy} \quad (51)$$

During the mapping interior points at the fluid wall interface are mapped to points on the y_2 axis. By the transformation of the right half-plane to the outside of the circle these points are mapped, together with their negative value of potential φ' , exactly to their original position if the y_1 coordinate would be reversed. For y symmetric ducts as considered here this is not a problem. Therefore, in any case the potential on Γ is known and given by

$$\varphi = -\varphi' = z. \quad (52)$$

Note, the solution obtained here results simply in the complex dipole $F = 1/z$ and corresponds to the solution of the inviscid flow initiated by a moving cylinder.

Results for the MHD core solution then are

$$\left. \begin{array}{l} \varphi_c = z, \\ u_c = 1, \\ a = 1. \end{array} \right\} \quad (53)$$

The core potential becomes simply a linear function along z . The core velocity is uniform and α is one.

It is known (see e.g. Chang and Lundgren (1961)) that in circular pipes with thin conducting walls or in ducts with perfectly conducting walls the velocity profile is of slug flow type in the whole core. Here, the slug flow profile in the core remains even if the duct walls are infinitely thick with finite conductivity.

The results discussed above do not apply, however, for ducts with sharp corners like rectangular ducts. The interior of ducts with polygonal cross section may be mapped of course by the Schwarz-Christoffel transformation to one half-plane with all corners on one of the ξ_2 axes. During the back transformation of the other half-plane to the exterior of the polygon the images of the corners not necessarily are mapped back to their initial position. Therefore, the a priori statement $\varphi_c = z$ does not apply and one has to expect interesting phenomena near sharp corners of ducts. The transformation of polygons involves fictive sources and sinks (logarithmic singularities near the corners). One has to expect that such singularities are reflected in the core solution for rectangular ducts. For references on conformal mapping see e.g. Betz (1964), Milne-Thomson (1974).

4.2 Square duct, diagonally aligned with the field

For the first example of a square duct the orientation is chosen with the diagonal of nondimensional length of 2 aligned with the magnetic field. Current streamlines and isolines of potential in the wall as well as in the cross section are displayed in figure 4. They are qualitatively similar to those obtained around a circular duct as just discussed in the previous subsection. Here, however, the isolines deviate clearly from circles, especially near the fluid-wall interface. Inside the cross section one can observe a concentration of isolines of potential near $z = 0$. The potential gradient profile along z is shown in figure 5. The profile of potential gradient $\partial_z \varphi_c$ can be interpreted directly as the profile of core velocity since $u_c = K(1 + \sigma_w^{-1} \partial_z \varphi_c)$. There is a possibility of an internal jet flow near $z = 0$. The velocity in the jet may exceed that of the mean flow by orders of magnitude. Internal jets as observed here are unknown from literature about MHD duct flows. The reason for such jets is a discontinuous source/sink distribution along the tangential direction s . Approaching the point $y(z)$ on Γ near $z = +\varepsilon$ as $\varepsilon \rightarrow 0$, the source intensity increases monotonically. Beyond $z = 0$ for $z = -\varepsilon$ the intensity of the sinks must balance the sources, $q(\varepsilon) = -q(-\varepsilon)$. At $z = 0$ the variation of q is not continuous. The strong increase in magnitude of the source/sink intensity near $z = 0$ is responsible for the formation of the internal jet. The internal jet is created by the solution of potential inside the wall and is therefore independent in width and magnitude of the Hartmann number.

On the other hand, a reversed flow near the sides at $z_{\pm} = \pm 1$ becomes possible if the wall conductivity falls below a certain value. With the highest resolution used ($n = 1000$) a value of $\partial_z \varphi_c(z_{\pm}) = -0.867$ was obtained. Therefore, reversed flow is expected to occur if $\sigma_w < 0.867$. The coefficient α for the pressure drop correlation becomes $\alpha = 1.187$.

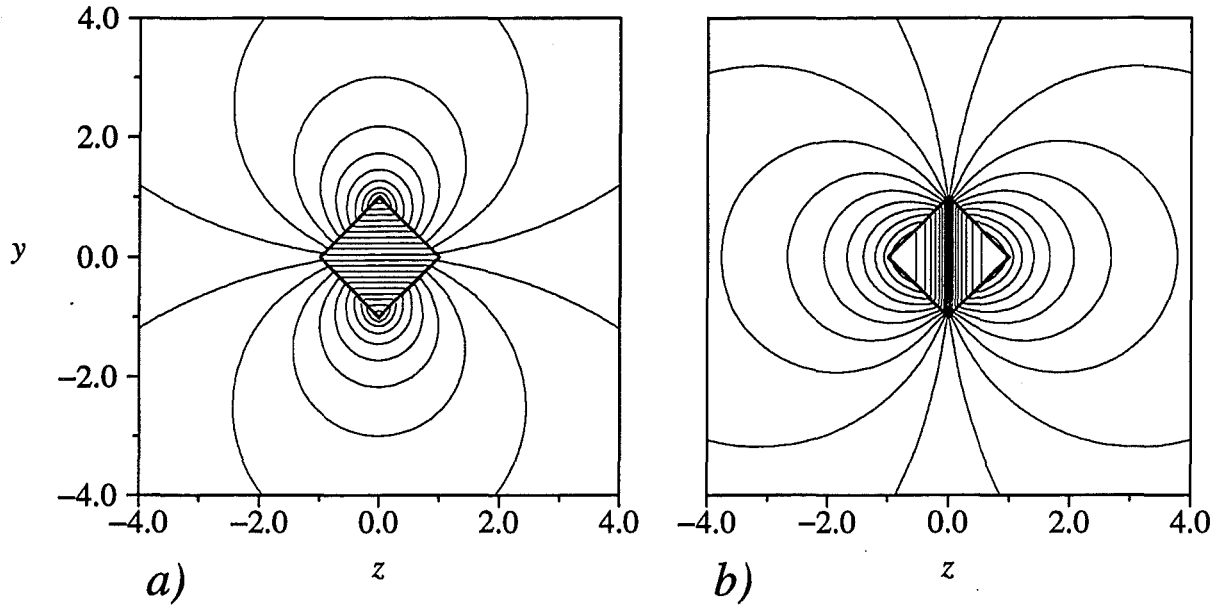


Figure 4: Isolines for current function (a) and potential (b) for the MHD flow in a square duct with infinitely thick walls. The duct is diagonally aligned with the magnetic field.

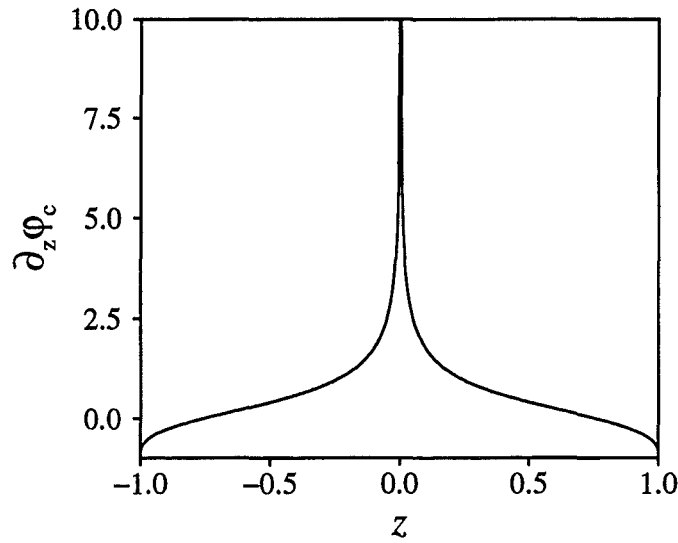


Figure 5: Plot of $\partial_z \varphi_c$ versus z for the flow in a square duct diagonally aligned with the field. From this plot one gets a good impression about the velocity profile which is given by $u_c = K(1 + \sigma_w^{-1} \partial_z \varphi_c)$. There is a possibility for a reversed flow near the sides if the wall conductivity σ_w is smaller than a specific value. Near $z = 0$ an internal jet is created.

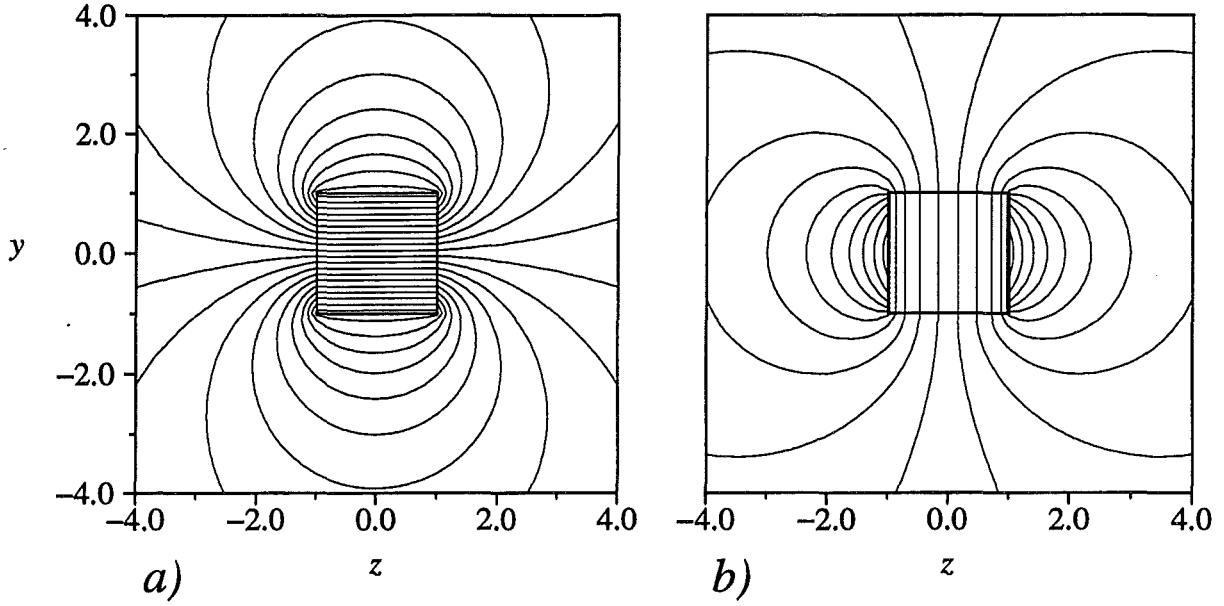


Figure 6: Isolines for current function (a) and potential (b) for the MHD flow in a square duct with infinitely thick walls. Two side walls of the duct are aligned with the magnetic field.

4.3 Square duct, side walls aligned with the field

The next example is the flow in a square duct, of which one pair of walls is aligned with the magnetic field. The current streamlines and isolines of potential in the wall and in the cross section are displayed in figure 6. The uniform current density created by the flow inside the duct enters the side wall. Near the sides, the currents change immediately their direction to close within the wall. If there is a y component of current in the wall this current creates a variation of potential along magnetic field lines. This becomes visible by considering isopotential lines near the sides. Some start and end at the same side wall, indicating that there is a higher/lower potential near $y = 0$ than near the Hartmann walls $y = \pm 1$. In the core, however, the potential remains uniform at the value as on the Hartmann wall at $y = \pm 1, z = \pm 1$. This fact leads to a jump of potential $\Delta\phi_s = K\sigma_w^{-1}\Delta\varphi_s = |\phi_w - \phi_c|$ across the side layers, giving rise to a high-velocity jet along the side wall. It has been shown that the flow rate carried by the side layer is already given, if the potential jump across the layer is known.

$$U_s = \frac{K}{\sigma_w} \Delta\varphi_s \text{ at } z = \pm 1. \quad (54)$$

Results for $\Delta\varphi_s$ are displayed in figure 7. The side layer jet here is more of elliptic shape than of parabolic one as it is the case for thin conducting walls. The total flow carried by both layers is $U_{s,total} = 2.13K/\sigma_w$.

The flow in the core $u_c = K(1 + \sigma_w^{-1}\partial_z\varphi_c)$ is determined by the potential gradient $\partial_z\varphi_c$ which is shown in figure 8. There is a possibility of a new type of high-velocity jet along side walls even within the inviscid core. A strong variation of core velocity with

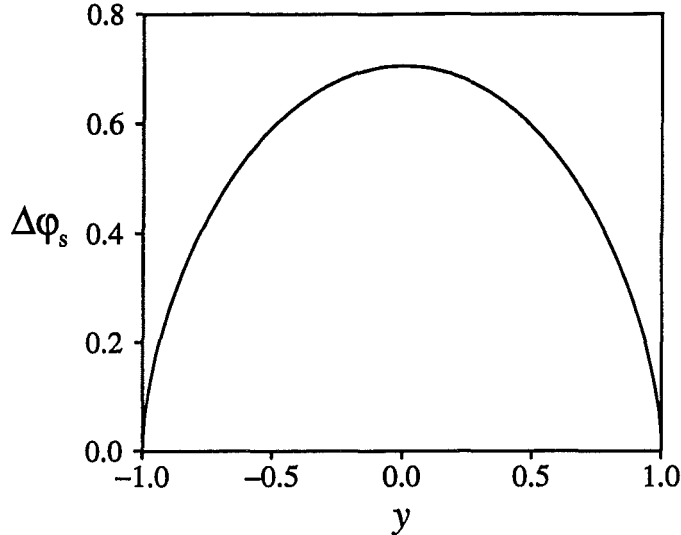


Figure 7: Jump of potential $\Delta\varphi_s$ across the side layer giving rise to high-velocity jets with flow rate $U_s = \frac{K}{\sigma_w} \Delta\varphi_s$. For poor conducting walls the flow in the layers reaches order unity

z is possible if the current density in the wall adjacent the fluid/wall interface varies along z . The strongest variation occurs of course near the corner, where a discontinuous source/sink distribution along s is needed to create the required electrical current conditions for the wall solution. Inviscid or inner layers have been observed for thin conducting ducts in a number of references (see e.g. Walker (1981), Bühler (1998)). In these references the inviscid layers are generated by an exchange of current between the thin conducting Hartmann walls. The conductivity of those Hartmann walls, specified by the wall conductance ratio $c = \sigma_w t$ with the nondimensional wall thickness t determines the thickness of the mentioned layers. The thickness there is determined as $\delta_{inviscid} \sim c^{1/2}$. Inviscid layers may appear also in rectangular ducts in the presence of a contact resistance between the fluid and the wall (Bühler and Molokov (1994)). In that case the inviscid layer thickness $\delta_{inviscid} \sim (M/\kappa)^{1/2}$ depends on the Hartmann number M and the nondimensional contact resistance κ . Bühler and Molokov (1993) argued that the discrepancy between classical experiments and theories for duct flows in well conducting channels (see the review published by Branover (1978) p 84-85) may have been created by a contact resistance between the fluid and the duct walls. The present analysis now suggests a second possible explanation namely the finite conductivity of the relatively thick walls used in those experiments..

In contrast, here, the conductivity of the wall or the Hartmann number M have no influence on the thickness of the observed inviscid layer. The thickness is on the order unity and affects a significant fraction of the core. The conductivity plays a role in so far as it determines the magnitude and flow rate which is proportional to K/σ_w .

The total flow rate carried by the core becomes $U_c = K(4 + 2.67\sigma_w^{-1})$. As σ_w becomes

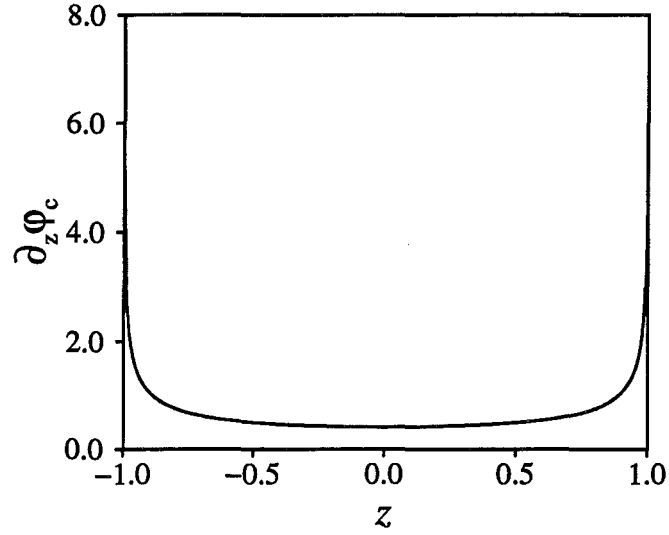


Figure 8: Variation of $\partial_z \varphi_c$ along z . The potential gradient determines the core velocity as $u_c = K (1 + \sigma_w^{-1} \partial_z \varphi_c)$. For moderate or small values of σ_w the core exhibits significantly higher velocities near the side walls than near the $z = 0$.

small, $\sigma_w \ll 1$, the flow carried by the core approaches 1.25 times the flow carried by the jets along the side walls. The pressure drop coefficient α finally becomes $\alpha = 1.19$.

5 Conclusions

The MHD flow in ducts with very thick walls has been investigated. Such ducts are elements of currently designed liquid-metal blankets for fusion reactors. The results have been obtained by the solution of an integral equation determining in a first step the complex potential for current inside the wall. The flow has been calculated using asymptotic methods valid at large Hartmann numbers M . For strong magnetic fields, $M \gg 1$, the flow exhibits a core where viscous effects can be disregarded. The inviscid core is surrounded by thin viscous layers called the Hartmann layers if there is a wall normal component of the magnetic field across these layers. Their thickness scales as $\delta_H \sim M^{-1}$. Near walls which are perfectly aligned with the field viscous side layers with typical scales $\delta_s \sim M^{-1/2}$ appear.

For circular ducts the potential becomes a linear function of the transverse coordinate and the flow is of slug type.

For square ducts where one diagonal is aligned with the magnetic field a high-velocity jet near the aligned diagonal is found. Such internal jets are unusual in known solutions of MHD duct flow problems.

For square ducts with one pair of walls aligned with the magnetic field high-velocity jets occur near the side walls. It is surprising that such jets exist even if the side walls are infinitely thick. The side layer jets are formed by two contributions. One part is created by the viscous correction to the core solution near the side wall just as in ducts with thin walls. The other part of the side layer jets is similar to the internal jet for case of the diagonal alignment and is part of the inviscid core. Even if these jets seem to be relatively thin their dimension is created by the characteristic dimensions of the duct and is therefore on the order unity.

It has been shown that for all ducts shapes discussed here the pressure gradient can be correlated by a simple formula

$$K = (1 + \sigma_w^{-1}\alpha)^{-1}, \quad (55)$$

where σ_w corresponds to the ratio of wall to fluid conductivity. The parameter α is near unity and depends only on the shape of the duct. This result is most important since in the past the MHD pressure drops in thick-walled ducts have been estimated by the pressure drop as in perfectly conducting channels. In engineering applications σ_w is rather unity than being infinite. This leads to a pressure drop approximately half as high as the old estimates or even lower.

References

- Betz, A.: 1964, *Konforme Abbildung*, Springer-Verlag.
- Branover, H.: 1978, *Magnetohydrodynamic flow in ducts*, Jhon Wiley & Sons, New York, Toronto.
- Bühler, L.: 1994, Magnetohydrodynamic flows in arbitrary geometries in strong, nonuniform magnetic fields.-a numerical code for the design of fusion reactor blankets, *Fusion Technology* **27**, 3–24.
- Bühler, L.: 1998, Laminar buoyant magnetohydrodynamic flow in vertical rectangular ducts, *Physics of Fluids*.
- Bühler, L. and Molokov, S.: 1993, Magnetohydrodynamic flows in ducts with insulating coatings, *Technical Report KfK 5103*, Kernforschungszentrum Karlsruhe.
- Bühler, L. and Molokov, S.: 1994, Magnetohydrodynamic flows in ducts with insulating coatings, *Magnetohydrodynamics* **30**(4), 439–447.
- Chang, C. and Lundgren, S.: 1961, Duct flow in magnetohydrodynamics, *ZAMP* **XII**, 100–114.
- Hunt, J. C. R.: 1965, Magnetohydrodynamic flow in rectangular ducts, *Journal of Fluid Mechanics* **21**, 577–590.
- Milne-Thomson, L.: 1974, *Theoretical Hydrodynamics*, fifth edn, The Mcacmillan Press LTD.
- Molokov, S.: 1993, Fully developed liquid-metal flow in multiple rectangular ducts in a strong uniform magnetic field, *European Journal of Mechanics, B/Fluids* **12**(6), 769–787.
- Molokov, S. and Bühler, L.: 1994, Liquid metal flow in a U-bend in a strong uniform magnetic field, *Journal of Fluid Mechanics* **267**, 325–352.
- Moon, T. J., Hua, T. Q. and Walker, J. S.: 1991, Liquid-metal flow in a backward elbow in the plane of a strong magnetic field, *Journal of Fluid Mechanics* **227**, 273–292.
- Roberts, P. H.: 1967, Singularities of Hartmann layers, *Proceedings of the Royal Society of London* **300**(A), 94–107.
- Shercliff, A.: 1956, The flow of conducting fluids in circular pipes under transverse magnetic fields, *Journal of Fluid Mechanics* **1**, 644–666.
- Ting, A., Hua, T. Q., Walker, J. S. and Picologlou, B. F.: 1993, Liquid-metal flow in a rectangular duct with thin metal walls and with a non-uniform magnetic field, *International Journal of Engineering Science* **31**(3), 357–372.
- Walker, J. S.: 1981, Magnetohydrodynamic flows in rectangular ducts with thin conducting walls, *Journal de Mécanique* **20**(1), 79–112.